A circadian-like gene network regulates heterochronic miRNA transcription in *C. elegans*

Brian Kinney[1]*, Shubham Sahu[2]*, Natalia Stec[1], Kelly Hills-Muckey[1], Dexter W. Adams[3,4], Jing Wang[1], Matt Jaremko[3], Leemor Joshua-Tor[3], Wolfgang Keil[2,†], Christopher M. Hammell[1,†]

[1]Cold Spring Harbor Laboratory, Cold Spring Harbor, NY 11724, USA.

[2]Institut Curie, Université PSL, Sorbonne Université, CNRS UMR168 Laboratoire Physico Chimie Curie, 75005 Paris, France.

[3]Howard Hughes Medical Institute, W. M. Keck Structural Biology Laboratory, Cold Spring Harbor Laboratory, Cold Spring Harbor, NY, 11724, USA

[4]Graduate Program in Genetics, Stony Brook University; Stony Brook, NY 11794, USA

*These authors contributed equally

[†]Correspondence: wolfgang.keil@curie.fr (W.K.); chammell@cshl.edu (C.M.H.) (lead contact)

Abstract:

Developmental robustness relies on precise control of the timing and order of cellular events. In *C. elegans*, the invariant sequence of post-embryonic cell fate specification is controlled by oscillatory patterns of heterochronic microRNA transcription that are phase-locked with the larval molting cycle[1-4]. How these transcriptional patterns are generated and how microRNA dosage is controlled is unknown. Here we show that transcriptional pulses of the *lin-4* heterochronic microRNA are produced by two nuclear hormone receptors, NHR-85 and NHR-23, whose mammalian orthologs, Rev-Erb and ROR, function in the circadian clock. While Rev-Erb and ROR play antagonistic roles in regulating once-daily transcription[5-7], we find that NHR-85 and NHR-23 bind cooperatively as heterodimers to *lin-4* regulatory elements to induce a single brief pulse of expression during each larval stage. We demonstrate that the timing and duration of *lin-4* transcriptional pulses are programmed by the phased overlap of NHR-85 and NHR-23 protein expression and that these regulatory interactions are post-transcriptionally controlled by LIN-42, the circadian Period ortholog in *C. elegans*. These findings suggest that an evolutionary rewiring of the circadian clock machinery is co-opted in nematodes to generate periodic transcriptional patterns that define cell fate progression.

Introduction

Many gene regulatory networks encode and read information controlling the tempo and order of developmental events. *C. elegans* postembryonic maturation is compartmentalized into four larval stages with distinct patterns of cell division, cell differentiation, and cuticle formation that are separated by molts[8]. The transition from one stage-specific pattern of cell division to the next is mediated by the accumulation of heterochronic microRNAs (miRNAs) that post-transcriptionally downregulate temporal identity target genes that define stage-specific gene expression patterns[9]. Hence, lower or higher dosages of heterochronic miRNAs result in precocious cellular transitions or reiteration of stage-specific cellular programs, respectively. The transcription of heterochronic microRNAs is periodic, peaking at specific phases of each larval molting cycle[1-4]. This suggests the existence of a clock-like system to coordinate their temporal expression with overall developmental progression.

Evidence suggests that LIN-42, the *C. elegans* ortholog of the circadian Period protein, is required for temporal patterning by directly modulating the dynamic features of heterochronic microRNA transcription[1,2,4]. Loss-of-function mutations in *lin-42* increase the amplitude and duration of cyclical heterochronic miRNA transcription, indicating that LIN-42, like its mammalian ortholog, functions as a transcriptional repressor[1,2,4]. Consequently, *lin-42* mutants develop precociously due to overaccumulation of heterochronic microRNAs[2,10]. While most core components of the heterochronic gene regulatory network are expressed in a graded temporal pattern, LIN-42 is highly dynamic, with a single peak of expression during each larval stage[2,10]. The similar molecular functions and expression dynamics between LIN-42 and mammalian Period suggest that a regulatory architecture akin to the one that generates the once-daily circadian transcriptional patterns in mammals may play a role in temporal cell fate specification in nematodes. Intriguingly, *C. elegans* lacks orthologs of CLOCK and BMAL1, the central transcription factors that drive oscillatory circadian transcription and the direct targets of Period repression. Thus, the mechanism by which LIN-42 modulates the transcriptional output of *C. elegans* heterochronic microRNAs is currently unknown.

Oscillatory *lin-4* transcription is pulsatile

Previous measurements of miRNA transcription used destabilized GFP reporters that must be transcribed, processed, and translated to visualize expression dynamics[2,11]. These features limit their temporal resolution. We used the MS2/MCP-GFP tethering system, where engineered RNA loops derived from MS2 bacteriophage and a co-expressed MS2 coat protein fused to green

68 fluorescent protein (MCP-GFP) can be concentrated and localized at a gene of interest by active
69 transcription (Fig.1a)[12]. We measured the transcriptional dynamics of the *lin-4* heterochronic miRNA
70 that is expressed periodically throughout all larval stages and down-regulates *lin-14* expression within
71 the heterochronic gene regulatory network early in development[11]. We generated a transgene
72 harboring 24 copies of a synthetic MS2 hairpin immediately downstream of the *lin-4* pre-miRNA (Fig.
73 1a and Extended Data Fig. 1a)[11,13]. This transgene rescues *lin-4* null allele phenotypes (Extended
74 Data Fig. 1b,c). We also ubiquitously expressed MCP-GFP to detect MS2-tagged RNAs and a
75 histone::mCherry fusion to locate nuclei (Extended Data Fig. 1a). Examination of transgenic animals
76 revealed that the formation of nuclear MCP-GFP foci occurred at each larval stage in somatic tissue
77 types known to transcribe *lin-4* (Fig. 1b). MCP-GFP foci were not observed in developing embryos (n
78 > 50) or in starvation arrested L1 larva (n = 23); consistent with the activation of *lin-4* transcription
79 after the initiation of larval development[14].

80 To directly determine the level of coordination of transcriptional programs, at single-cell
81 resolution, across cell and tissue types in living animals, we used our microfluidics-based platform[15]
82 for long-term imaging of *C. elegans* larvae harboring *lin-4::24xMS2/MCP-GFP* system. We quantified
83 expression dynamics in hypodermal cells where the timing of transcriptional activity can be accurately
84 assessed in relation to the occurrence of stage-specific cell division patterns[8]. We screened for
85 periods of *lin-4* transcriptional activity by imaging at 15min time intervals from the first larval stage
86 (L1) to the mid-L4 stage (~60h) (n>10). *lin-4::24xMS2* transcription was highly pulsatile, with a single
87 transcriptional episode of ~45-90min in each cell during each larval stage, followed by long periods
88 of inactivity (>8hrs at 20°C) (Fig. 1c). Transcriptional activation across cells within the hypodermis
89 was highly concordant, exhibiting similar transcriptional on and off times for all *lin-4::24xMS2* loci (Fig.
90 1e). For instance, during the mid-L3 stage, the appearance of *lin-4::24xMS2* expression throughout
91 the hypodermis generally occurred within minutes of the first vulval precursor cell (VPC) divisions
92 (P3.p or P4.p) and were completed by the divisions of remaining VPCs (P5.p-P7.p) (n = 15) (Fig. 1c).

93 To determine how similar the transcriptional dynamics in individual cells within the hypodermis
94 are, we performed short-term imaging time courses (<6h) at 4min intervals in staged larvae. During
95 transcriptional episodes, we detected near synchronous accumulation of MCP-GFP foci at each
96 hypodermal *lin-4::24xMS2* locus for 60-90 minutes (Fig. 1d,e, Suppl. Movie 1,2) (>15 animals). We
97 found no signs of "bursty" transcription[16] as MCP-GFP foci were continuously maintained at each *lin-*
98 *4::24xMS2* transgene for the entire transcriptional episode (Suppl. Movie 1,2). These features were
99 independent of the number of *lin-4::24xMS2* loci per nucleus as cell types that undergo
100 endoreduplication (i.e., hyp7 cells) exhibited MCP-GFP foci dynamics indistinguishable from diploid

101 cells (Fig. 1d). The dynamic features of *lin-4::24xMS2* expression in hypodermal cells were similar
102 across different developmental stages (Fig. 1e) suggesting that the same regulatory programs
103 controlling *lin-4* transcription were repeated at each larval stage. Pulsatile transcription also occurs in
104 a broad array of additional cell types that normally express *lin-4* (including the pharynx and intestinal
105 cells) (Extended Data Fig. 2). Therefore, the gene regulatory network that generates *lin-4*
106 transcriptional pulses at each stage of development organizes the timing, amplitude and duration of
107 transcription in a highly reproducible manner.

108 **NHR-85 and NHR-23 function cooperatively**

109 Full transcriptional activation of *lin-4* requires a conserved upstream regulatory element, the
110 Pulse Control Element (PCE), located ~2.8kb upstream of the *lin-4* sequence [11]. We performed a
111 yeast-one-hybrid screen to discover TFs that bind this regulatory region using the entire 514bp PCE
112 as bait. We identified three TFs that specifically bound the PCE (BLMP-1, NHR-23, and NHR-85)
113 (Fig. 2a). BLMP-1 controls the amplitude of *lin-4* expression and functions as a pioneer factor to
114 decompact the *lin-4* locus throughout development [11]. *nhr-85* and *nhr-23* encode two nuclear
115 hormone receptors (NHRs) that are the closest nematode orthologs of human circadian TFs Rev-Erb
116 and ROR, respectively (Fig. 2b). NHR-23 expression cycles with the larval molts and has been
117 implicated in controlling the pace of larval development [17-19]. Furthermore, *nhr-23* and the terminal
118 heterochronic miRNA, *let-7*, genetically interact to mutually limit supernumerary molts during
119 adulthood [18,20]. Analysis of publicly available ChIP-seq data indicated that all three TFs interact *in vivo*
120 with *lin-4* regulatory sequences (Fig. 2a), and their binding sites are enriched in the promoters of
121 cyclically expressed mRNAs and other heterochronic miRNAs (Extended Data Fig. 3) (table S1 and
122 S2).

123 Nuclear hormone receptors often bind cooperatively as homo- or hetero-dimeric complexes
124 at closely spaced cis-regulatory DNA elements [21-23]. Several features of NHR-85$^{Rev-Erb}$, NHR-23^{ROR,}
125 and the *lin-4* PCE suggest that this may also be the case for *lin-4* transcription. First, NHR-85$^{Rev-Erb}$
126 and NHR-23^{ROR} share significant sequence homology within their C4-type Zinc finger DNA-binding
127 domains, suggesting they bind similar sites (Fig. 2c) [24]. Second, we found that NHR-85$^{Rev-Erb}$ and
128 NHR-23^{ROR} heterodimerize in yeast two-hybrid assays and *in vitro* with high affinity (5.8 +/- 2.2 nM
129 K_D (Fig. 2d,e)). Third, sequences within the PCE element contain direct GGTCA repeats that are
130 predicted binding sites of NHR-85$^{Rev-Erb}$ and NHR-23^{ROR} (Fig. 2f and g). Fourth, we found that
131 concentrations of NHR-23^{ROR} that were insufficient to bind the PCE alone were dramatically
132 stimulated by the addition of NHR-85$^{Rev-Erb}$, indicating cooperative binding (Fig. 2h, i). Supporting this,

133 NHR-85$^{Rev-Erb}$ alone could not bind *lin-4* PCE DNA fragments (Extended Data Fig. 4c). Finally, the
134 cooperative binding of NHR-85$^{Rev-Erb}$ and NHR-23^{ROR} required both GGTCA repeats, suggesting they
135 bind closely spaced regulatory elements as a heterodimer (Fig. 2h).

136 **NHR-85/NHR-23 expression coincides with *lin-4* transcription**

137 We quantified mRNA and protein expression during post-embryonic development to
138 determine how NHR-85, NHR-23, and LIN-42 expression patterns may contribute to the regulation of
139 oscillatory lin-4 transcription. Expression of *nhr-85* begins from an L1-stage arrest with a pulse of
140 transcription that is followed by a monotonic expression pattern for the remaining larval stages (Fig.
141 3a). In contrast, *nhr-23* and *lin-42* mRNAs were expressed in phased, high-amplitude oscillatory
142 patterns (Fig. 3a). We next explored the temporal dynamics of the corresponding proteins, by
143 quantifying the expression of endogenously-tagged alleles during the L4 stage, where changes in
144 vulval morphogenesis can be directly correlated with developmental age [25]. NHR-23^{ROR}::mScarlet
145 and LIN-42^{Period}::GFP are dynamically expressed in all hypodermal cells, with a single peak of
146 expression that matched the phased expression of their mRNAs (Fig. 3c). We also found that NHR-
147 85$^{Rev-Erb}$::GFP expression was highly dynamic during these periods, indicating substantial post-
148 transcriptional regulation of expression in the L2-L4 stages of development. Specifically, peak
149 expression of NHR-85$^{Rev-Erb}$::GFP occurred at ecdysis (shortly before NHR-23^{ROR}::mScarlet onset),
150 becomes undetectable by the L4.3 stage of development, and resumes expression at the L4.6 stage
151 in an antiphasic manner to the expression pattern of LIN-42^{Period}::YFP (Fig. 3b). Highly similar phased
152 expression patterns of these proteins are also maintained in L4-staged vulval tissues (Fig. 3c) as well
153 as in L3-staged hypodermal cells and VPCs (Fig. 3c-e).

154 Since NHR-85$^{Rev-Erb}$ and NHR-23^{ROR} heterodimerize and bind cooperatively to regions of the
155 *lin-4* enhancer that control dynamic transcription, we hypothesized that the 60-90min pulses of *lin-4*
156 transcription might only occur in the short window of each larval stage where NHR-85$^{Rev-Erb}$ and NHR-
157 23^{ROR} are co-expressed. To compare the timing of these events, we examined MCP-GFP localization
158 in vulval cells during the L3 and L4 stages, where the rapid, stereotyped vulval cell division patterns[15]
159 and changes in morphology[25] enable precise determination of the timing of *lin-4::24xMS2*
160 transcription and TF expression dynamics. We found a correspondence between NHR-85$^{Rev-Erb}$ and
161 NHR-23^{ROR} co-expression and *lin-4::24xMS2* transcription in both vulval and hypodermal cells (Fig.
162 3d,e). While the expression of both nuclear receptors is phased, the transient expression of the *lin-*
163 *4::24xMS2* transgene only occurs during the brief period when both NHRs are expressed. The timing
164 of NHR-85$^{Rev-Erb}$ post-transcriptional downregulation is also concurrent with the onset of LIN-42^{Period}

165 expression in VPCs and hypodermal cells (Fig. 3c-e). This suggests that the dynamic patterns of
166 these TFs control the timing and duration of *lin-4* transcriptional pulses.

167

168 **LIN-42^{Period} posttranscriptionally represses NHR-85**

169 Human Per2 (PERIOD2) protein interacts with multiple mammalian NHRs (including Rev-Erb)
170 to modulate their transcriptional activity [26]. To test whether LIN-42^{Period} physically interacts with either
171 NHR-85$^{Rev\text{-}Erb}$ or NHR-23^{ROR}, we used two-hybrid assays [27]. We found that both major LIN-42 isoforms
172 interact with NHR-85$^{Rev\text{-}Erb}$ but not NHR-23^{ROR} (Fig. 4a). We mapped the regions of LIN-42^{Period} that
173 are required for NHR-85$^{Rev\text{-}Erb}$ binding and found that a minimal 51aa fragment present in both major
174 LIN-42^{Period} isoforms is sufficient to mediate interactions (Fig. 5a). This domain is distinct from the
175 interaction motifs implicated in mammalian Per2 and Rev-Erb [26]. Because Per2 has been shown to
176 interact with many mammalian NHRs, we extended our two-hybrid analysis of LIN-42^{Period} interactors
177 to determine if LIN-42^{Period} also binds additional NHRs. We performed two-hybrid experiments
178 between LIN-42^{Period} isoforms and 241 of the remaining 282 encoded *C. elegans* NHRs. We identified
179 65 NHRs that physically interact with LIN-42^{Period}(Extended Data Fig. 5a,b). The additional interacting
180 NHRs included DAF-12, which regulates the expression of the *let-7*-family of miRNAs and controls
181 dauer development[28-30], and NHR-14^{HNF4a}, NHR-69^{HNF4a}, and NHR-119 PPARα (Extended Data Fig.
182 5a,b) whose orthologs are also bound by Per2 [26]. These findings suggest that many physical
183 interactions between Period orthologs have been maintained since the divergence of nematodes and
184 man and are, therefore, likely functional.

185 Given the physical interaction between NHR-85$^{Rev\text{-}Erb}$ and LIN-42^{Period}, we asked whether
186 NHR-85$^{Rev\text{-}Erb}$ expression was required for the precocious phenotypes seen in *lin-42(lf)* mutants (*lin-*
187 *42(n1089)*). We found that *lin-42(lf)* heterochronic phenotypes are partially ameliorated by removing
188 *nhr-85* function. Specifically, the precocious expression of adult-specific reporters (e.g., *col-19::GFP)*
189 in both seam and hyp7 cells observed in *lin-42(lf)* mutants is suppressed by *nhr-85* deletion; leaving
190 weak expression in seam cells in double mutants, while precocious deposition of adult alae was not
191 suppressed (Fig. 4b). To examine whether LIN-42^{Period} regulates NHR-85$^{Rev\text{-}Erb}$ temporal expression,
192 we compared the dynamics of NHR-85$^{Rev\text{-}Erb}$::GFP (and NHR-23^{ROR}::mScarlet) levels in wild-type and
193 *lin-42(lf)* mutants. We found that the expression of NHR-85$^{Rev\text{-}Erb}$ is altered in two ways by the *lin-42*
194 mutation. First, the expression of NHR-85$^{Rev\text{-}Erb}$::GFP is ~2.3x more abundant at the beginning of the
195 L4 stage in *lin-42* mutants when compared to wild-type animals (Fig. 4c,d). More importantly, the
196 periodic dampening of NHR-85$^{Rev\text{-}Erb}$ expression that usually occurs by the L4.2 stage of vulval

197 morphogenesis (Fig. 3c,d) is altered in *lin-42(lf)* mutants. Specifically, NHR-85$^{Rev\text{-}Erb}$::GFP expression
198 perdures into the L4.4 stage *lin-42(lf)* animals (Fig. 4c,d). Mutations in *lin-42* do not alter the onset or
199 duration of NHR-23^{ROR}::mScarlet accumulation in hypodermal or vulval cells. This suggests that LIN-
200 42 regulates *lin-4* transcriptional output by controlling the duration of NHR-85$^{Rev\text{-}Erb}$/NHR-23^{ROR}
201 heterodimeric complex formation in a manner that directly correlates with NHR-85 abundance.

202 Given the above hypothesis, we anticipated that specific features of *lin-4* transcriptional pulses
203 would be altered in *lin-42* mutants. While most wild-type seam cells exhibit MCP-GFP foci during
204 each larval stage (76%; n=66 nuclei), the percentage of seam cells showing detectable *lin-4*
205 transcription is dramatically increased in *lin-42* mutants (100%; n=58 nuclei). This indicates that *lin-*
206 *42* normally dampens *lin-4* transcriptional pulses in wild-type animals. In addition to elevating the
207 likelihood that *lin-4::24xMS2* transcription is above a threshold sufficient to generate measurable
208 MCP-GFP foci, *lin-42(lf)* mutations lead to an increase in the intensity of MCP-GFP foci indicating
209 that LIN-42^{Period} normally also limits the rate of transcriptional activation of the *lin-4* locus (Fig. 4e).
210 Time course experiments also revealed that overall duration of transcription events in lateral seam
211 cells was ~2.2 times longer in *lin-42* mutants compared to wild-type (Fig. 4e). Consistent with our
212 hypothesis that the duration of *lin-4* transcription is dependent on the duration of NHR-85$^{Rev\text{-}Erb}$
213 expression, the transcriptional onset of *lin-4::24xMS2* occurs earlier in L3 staged *lin-42* mutants and
214 inappropriately extended through both the first and second Pn.p divisions (Fig. 4f).

215 While *nhr-85(0)* mutants did not misexpress adult-specific reporters (Fig. 5b), high-resolution
216 imaging of VPC divisions and *lin-4::24xMS2* expression indicate two features of developmental timing
217 were altered. In wild-type animals, transcriptional pulses of *lin-4::24xMS2* are both robust and
218 concordant in adjacent wild-type VPCs (Figs. 4g & 1c). In contrast, MCP-GFP foci in *nhr-85(0)*
219 mutants begin to accumulate at the same relative phase of L3-stage VPC development but are
220 dimmer and only transiently observed (Fig. 4g). Second, under identical imaging conditions, the rapid
221 and highly coordinated VPC divisions observed in wild-type animals is altered in *nhr-85(0)* mutants
222 with some P5.p and P7.p dividing hours after the first P6.p division (Fig. 4g). These results indicate
223 that NHR-85 functions to enhance the robustness of temporally regulated processes during
224 development and that some level of *lin-4* transcription occurs without NHR-85$^{Rev\text{-}Erb}$, perhaps driven
225 by NHR-23^{ROR} alone. RNAi-mediated depletion of *nhr-23* activity in wild-type animals resulted in mild
226 heterochronic phenotypes (Extended Data Fig. 6). Consistent with the hypothesis that NHR-23 and
227 NHR-85 function cooperatively to control temporal regulation, the penetrance of these phenotypes
228 was enhanced when *nhr-23* was also depleted in *nhr-85(0)* animals (Extended Data Fig. 6).

229

Discussion

This study reveals the gene regulatory network controlling *lin-4* transcriptional pulses. This network shares integral components with the human circadian clock but exhibits essential differences in its regulatory architecture. In the circadian clock regulatory network, transcription factors CLOCK and BMAL1 generate rhythmic expression patterns of clock control genes (CCGs) [31-34] (Fig. 5h), including two core transcriptional repressors, Period and CRY as well as NHR genes Rev-Erb and ROR. Negative feedback on CLOCK/BMAL1 expression by Period/CRY heterodimers is essential for the proper generation of circadian rhythms. Rev-Erb and ROR modulate CLOCK and BMAL1 expression through opposing transcriptional activities (Fig. 4h) [5-7] but are dispensable for the generation of circadian oscillations [35]. Instead of CLOCK and BMAL1, which are lacking in the *C. elegans* genome, we propose here that the worm orthologs of Rev-Erb and ROR compose the central transcription factors of the hypodermal developmental clock (Fig. 5h). In contrast to their antagonistic roles in the circadian clock, *C. elegans* NHR-85$^{\text{Rev-Erb}}$ and NHR-23^{ROR} heterodimerize and work cooperatively to induce transcriptional pulses (Fig. 4h). The evolutionary rewiring of this interaction results in the phased expression of NHR-85$^{\text{Rev-Erb}}$ and NHR-23^{ROR} generating a short temporal window for these proteins to cooperativity promote transcription. This enables transcription to be precisely dosed and timed at each larval stage. This rewiring also provides a direct physical link to the conserved opposing arm of the clock, LIN-42^{Period}, which binds to NHR-85$^{\text{Rev-Erb}}$ to control NHR-85$^{\text{Rev-Erb}}$ expression post-transcriptionally (Fig. 4h). Additional physical and functional interactions between Period orthologs and conserved NHRs are maintained in the mammalian and *C. elegans* systems [26,28] and suggest that *C. elegans* NHRs, in addition to NHR-85$^{\text{Rev-Erb}}$, may also function in temporal patterning.

While NHR-85$^{\text{Rev-Erb}}$/NHR-23^{ROR} heterodimeric complexes generate pulses of *lin-4* transcription, NHR-23^{ROR} may play a more pervasive role in coordinating periodic transcription with overall animal development. Unlike *nhr-85*, *nhr-23* is an essential gene, and *nhr-23(0)* worms arrest during late embryogenesis/hatching, a time when oscillatory transcription begins[17,36,37]. Depletion of NHR-23^{ROR} during post-embryonic development results in highly penetrant larval arrest phenotypes [38]. These arrests prevent somatic cell proliferation/differentiation, occur at the beginning of each larval stage, and correlate with the developmental periods where NHR-23^{ROR} expression peaks[38]. While the developmental arrest in NHR-23^{ROR}-depleted animals makes it unfeasible to measure changes in transcription for individual genes, these arrests resemble post-embryonic developmental checkpoints where somatic cell proliferation and cyclical gene expression patterns (including *lin-4*) are halted during acute food removal/starvation [11,39]. Starvation-induced checkpoints are mediated through the

264 regulation of the conserved insulin signaling pathway, which generates various sterol-derived
265 hormones [40]. These hormones may serve as ligands for individual NHRs and provide a mechanism
266 to organize global gene expression patterns. This type of coordination may underly one mechanism
267 *C. elegans* larvae employ to generate identical developmental outcomes in diverse and rapidly
268 changing environments.

269

REFERENCES

1 Van Wynsberghe, P. M. & Pasquinelli, A. E. Period homolog LIN-42 regulates miRNA transcription to impact developmental timing. *Worm* **3**, e974453, doi:10.4161/21624054.2014.974453 (2014).

2 Perales, R., King, D. M., Aguirre-Chen, C. & Hammell, C. M. LIN-42, the Caenorhabditis elegans PERIOD homolog, Negatively Regulates MicroRNA Transcription. *PLoS genetics* **10**, e1004486, doi:10.1371/journal.pgen.1004486 (2014).

3 Kim, D. h., Grün, D. & van Oudenaarden, A. Dampening of expression oscillations by synchronous regulation of a microRNA and its target. *Nat Genet* **45**, 1337-1344, doi:10.1038/ng.2763 (2013).

4 McCulloch, K. A. & Rougvie, A. E. Caenorhabditis elegans period homolog lin-42 regulates the timing of heterochronic miRNA expression. *Proceedings of the National Academy of Sciences of the United States of America* **111**, 15450-15455, doi:10.1073/pnas.1414856111 (2014).

5 Preitner, N. *et al.* The orphan nuclear receptor REV-ERBalpha controls circadian transcription within the positive limb of the mammalian circadian oscillator. *Cell* **110**, 251-260, doi:10.1016/s0092-8674(02)00825-5 (2002).

6 Ueda, H. R. *et al.* A transcription factor response element for gene expression during circadian night. *Nature* **418**, 534-539, doi:10.1038/nature00906 (2002).

7 Sato, T. K. *et al.* A functional genomics strategy reveals Rora as a component of the mammalian circadian clock. *Neuron* **43**, 527-537, doi:10.1016/j.neuron.2004.07.018 (2004).

8 Sulston, J. E. & Horvitz, H. R. Post-embryonic cell lineages of the nematode, Caenorhabditis elegans. *Developmental biology* **56**, 110-156. (1977).

9 Ambros, V. MicroRNAs and developmental timing. *Current opinion in genetics & development* **21**, 511-517, doi:10.1016/j.gde.2011.04.003 (2011).

10 Jeon, M., Gardner, H. F., Miller, E. A., Deshler, J. & Rougvie, A. E. Similarity of the C. elegans developmental timing protein LIN-42 to circadian rhythm proteins. *Science* **286**, 1141-1146 (1999).

11 Stec, N. *et al.* An Epigenetic Priming Mechanism Mediated by Nutrient Sensing Regulates Transcriptional Output during C. elegans Development. *Curr Biol* **31**, 809-826 e806, doi:10.1016/j.cub.2020.11.060 (2021).

12 Tutucci, E. *et al.* An improved MS2 system for accurate reporting of the mRNA life cycle. *Nat Methods* **15**, 81-89, doi:10.1038/nmeth.4502 (2018).

13 Bracht, J. R., Van Wynsberghe, P. M., Mondol, V. & Pasquinelli, A. E. Regulation of lin-4 miRNA expression, organismal growth and development by a conserved RNA binding protein in C. elegans. *Developmental biology* **348**, 210-221, doi:10.1016/j.ydbio.2010.10.003 (2010).

14 Feinbaum, R. & Ambros, V. The timing of lin-4 RNA accumulation controls the timing of postembryonic developmental events in Caenorhabditis elegans. *Developmental biology* **210**, 87-95. (1999).

15 Keil, W., Kutscher, L. M., Shaham, S. & Siggia, E. D. Long-Term High-Resolution Imaging of Developing C. elegans Larvae with Microfluidics. *Developmental cell*, doi:10.1016/j.devcel.2016.11.022 (2016).

16 Larson, D. R., Singer, R. H. & Zenklusen, D. A single molecule view of gene expression. *Trends in cell biology* **19**, 630-637, doi:10.1016/j.tcb.2009.08.008 (2009).

17 Kostrouchova, M., Krause, M., Kostrouch, Z. & Rall, J. E. Nuclear hormone receptor CHR3 is a critical regulator of all four larval molts of the nematode Caenorhabditis elegans. *Proceedings of the National Academy of Sciences of the United States of America* **98**, 7360-7365, doi:10.1073/pnas.131171898 (2001).

18 Patel, R., Galagali, H., Kim, J. K. & Frand, A. R. Feedback between a retinoid-related nuclear receptor and the let-7 microRNAs controls the pace and number of molting cycles in C. elegans. *Elife* **11**, doi:10.7554/eLife.80010 (2022).

19 MacNeil, L. T., Watson, E., Arda, H. E., Zhu, L. J. & Walhout, A. J. M. Diet-induced developmental acceleration independent of TOR and insulin in C. elegans. *Cell* **153**, 240-252, doi:10.1016/j.cell.2013.02.049 (2013).

20 Hayes, G. D., Frand, A. R. & Ruvkun, G. The mir-84 and let-7 paralogous microRNA genes of Caenorhabditis elegans direct the cessation of molting via the conserved nuclear hormone receptors NHR-23 and NHR-25. *Development* **133**, 4631-4641, doi:10.1242/dev.02655 (2006).

21 Forman, B. M., Umesono, K., Chen, J. & Evans, R. M. Unique response pathways are established by allosteric interactions among nuclear hormone receptors. *Cell* **81**, 541-550, doi:10.1016/0092-8674(95)90075-6 (1995).

22 Perlmann, T., Umesono, K., Rangarajan, P. N., Forman, B. M. & Evans, R. M. Two distinct dimerization interfaces differentially modulate target gene specificity of nuclear hormone receptors. *Mol Endocrinol* **10**, 958-966, doi:10.1210/mend.10.8.8843412 (1996).

23 Rastinejad, F., Perlmann, T., Evans, R. M. & Sigler, P. B. Structural determinants of nuclear receptor assembly on DNA direct repeats. *Nature* **375**, 203-211, doi:10.1038/375203a0 (1995).

24 Burris, T. P. Nuclear hormone receptors for heme: REV-ERBalpha and REV-ERBbeta are ligand-regulated components of the mammalian clock. *Mol Endocrinol* **22**, 1509-1520, doi:10.1210/me.2007-0519 (2008).

25 Mok, D. Z. L., Sternberg, P. W. & Inoue, T. Morphologically defined sub-stages of C. elegans vulval development in the fourth larval stage. *BMC developmental biology* **15**, 26, doi:10.1186/s12861-015-0076-7 (2015).

26 Schmutz, I., Ripperger, J. A., Baeriswyl-Aebischer, S. & Albrecht, U. The mammalian clock component PERIOD2 coordinates circadian output by interaction with nuclear receptors. *Genes Dev* **24**, 345-357, doi:10.1101/gad.564110 (2010).

27 Walhout, A. J., Boulton, S. J. & Vidal, M. Yeast two-hybrid systems and protein interaction mapping projects for yeast and worm. *Yeast* **17**, 88-94, doi:10.1002/1097-0061(20000630)17:2<88::AID-YEA20>3.0.CO;2-Y (2000).

28 Tennessen, J. M., Opperman, K. J. & Rougvie, A. E. The C. elegans developmental timing protein LIN-42 regulates diapause in response to environmental cues. *Development* **137**, 3501-3511, doi:10.1242/dev.048850 (2010).

29 Hammell, C. M., Karp, X. & Ambros, V. A feedback circuit involving let-7-family miRNAs and DAF-12 integrates environmental signals and developmental timing in Caenorhabditis elegans. *Proceedings of the National Academy of Sciences of the United States of America* **106**, 18668-18673, doi:10.1073/pnas.0908131106 (2009).

30 Bethke, A., Fielenbach, N., Wang, Z., Mangelsdorf, D. J. & Antebi, A. Nuclear hormone receptor regulation of microRNAs controls developmental progression. *Science* **324**, 95-98 (2009).

31 Bunger, M. K. *et al.* Mop3 is an essential component of the master circadian pacemaker in mammals. *Cell* **103**, 1009-1017, doi:10.1016/s0092-8674(00)00205-1 (2000).

32 Hogenesch, J. B., Gu, Y. Z., Jain, S. & Bradfield, C. A. The basic-helix-loop-helix-PAS orphan MOP3 forms transcriptionally active complexes with circadian and hypoxia factors. *Proc Natl Acad Sci U S A* **95**, 5474-5479, doi:10.1073/pnas.95.10.5474 (1998).

33 King, D. P. *et al.* Positional cloning of the mouse circadian clock gene. *Cell* **89**, 641-653, doi:10.1016/s0092-8674(00)80245-7 (1997).

34 Reick, M., Garcia, J. A., Dudley, C. & McKnight, S. L. NPAS2: an analog of clock operative in the mammalian forebrain. *Science* **293**, 506-509, doi:10.1126/science.1060699 (2001).

35 Francois, P., Despierre, N. & Siggia, E. D. Adaptive temperature compensation in circadian oscillations. *PLoS Comput Biol* **8**, e1002585, doi:10.1371/journal.pcbi.1002585 (2012).

36 Meeuse, M. W. *et al.* Developmental function and state transitions of a gene expression oscillator in Caenorhabditis elegans. *Mol Syst Biol* **16**, e9498, doi:10.15252/msb.20209498 (2020).

37 Hendriks, G.-J., Gaidatzis, D., Aeschimann, F. & Großhans, H. Extensive Oscillatory Gene Expression during C. elegans Larval Development. *Mol Cell* **53**, 380-392, doi:10.1016/j.molcel.2013.12.013 (2014).

38 Johnson, L. C. *et al.* NHR-23 activity is necessary for developmental progression and apical extracellular matrix structure and function. *bioRxiv*, 2021.2010.2027.465992, doi:10.1101/2021.10.27.465992 (2022).

39 Schindler, A. J., Baugh, L. R. & Sherwood, D. R. Identification of late larval stage developmental checkpoints in Caenorhabditis elegans regulated by insulin/IGF and steroid hormone signaling pathways. *PLoS genetics* **10**, e1004426, doi:10.1371/journal.pgen.1004426 (2014).

40 Baugh, L. R. & Hu, P. J. Starvation Responses Throughout the Caenorhabditis elegans Life Cycle. *Genetics* **216**, 837-878, doi:10.1534/genetics.120.303565 (2020).

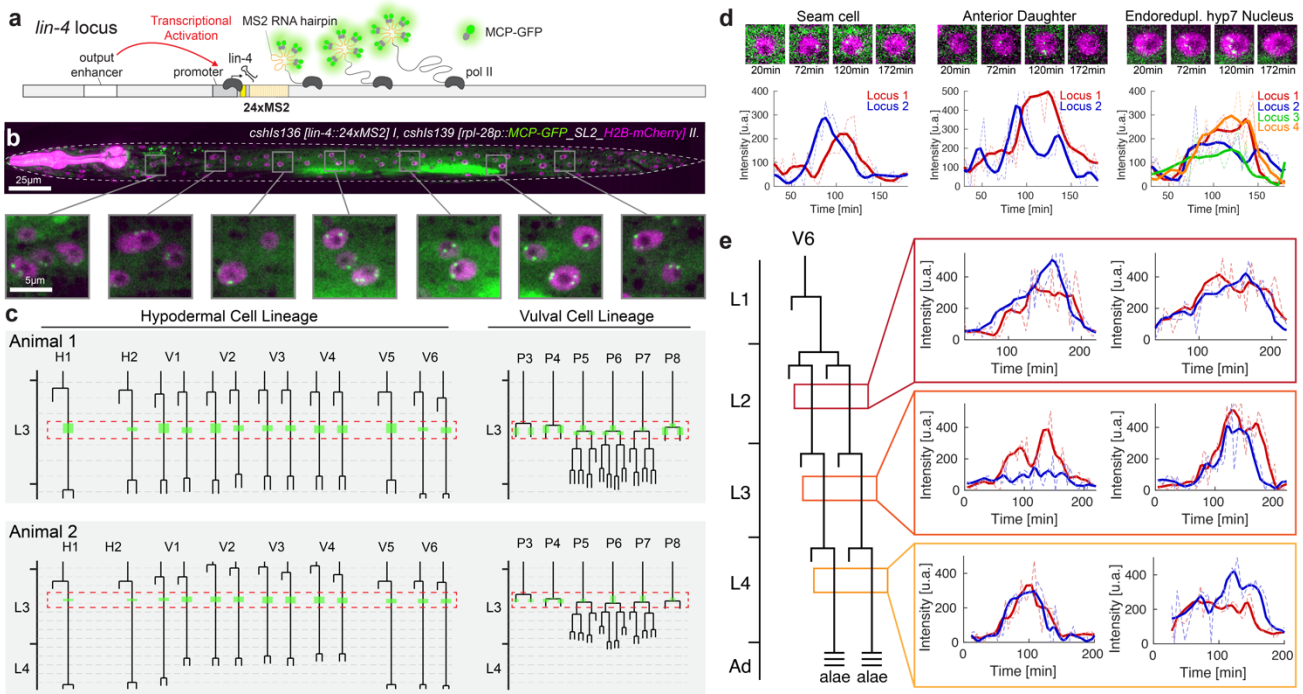

Fig. 1. *lin-4* transcription is highly pulsatile at each larval stage. (**a**) The MS2/MCP system is composed of an MS2 coat protein GFP fusion (MCP-GFP) which can bind to MS2 RNA hairpins engineered into primary miRNA transcripts. (**b**) Image of mid-L3 staged larva and magnified insets showing MCP-GFP spots in hypodermal cells along the anteroposterior axis. (**c**) Two examples of L3/L4 hypodermal and vulval precursor cell lineages, with overlayed expression patterns indicating when MCP-GFP foci were visible in each lineage. Red boxes show the temporal region where coordinated *lin-4* transcription is observed. Dashed horizontal grey bars indicate hours. (**d**) Snapshots of individual seam cell and hyp7 cell expression trajectories from L3-staged animals. (**e**) Expression traces in pairs of V6.p seam cells from L2, L3, and L4 staged animals.

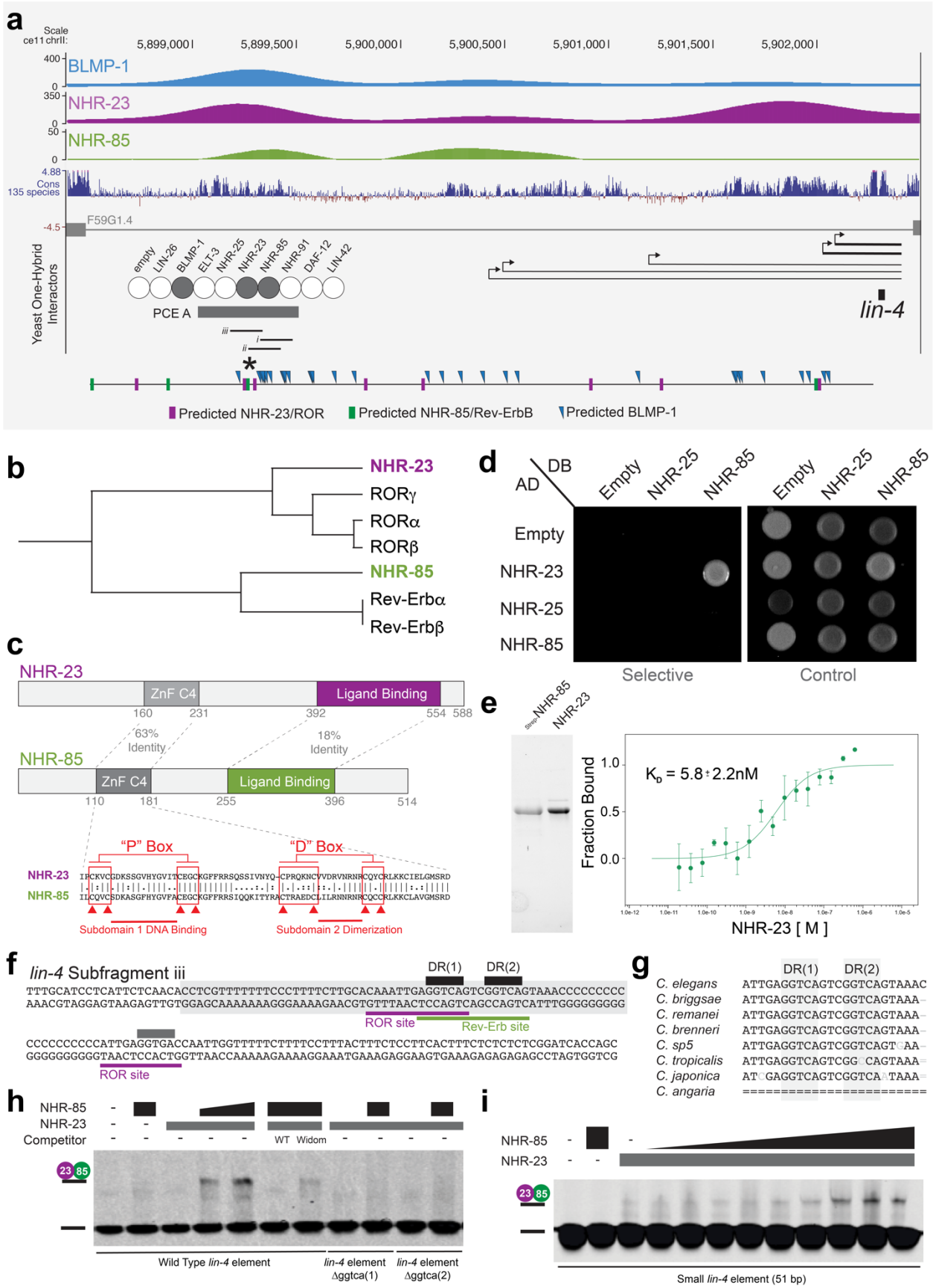
a
Scale
ce11 chrII:
5,899,000
5,899,500
5,900,000
5,900,500
5,901,000
5,901,500
5,902,000
BLMP-1
NHR-23
NHR-85
Cons
135 species
F59G1.4
Yeast One-Hybrid Interactors
empty
LIN-26
BLMP-1
ELT-3
NHR-25
NHR-23
NHR-85
NHR-91
DAF-12
LIN-42
PCE A
lin-4
Predicted NHR-23/ROR
Predicted NHR-85/Rev-ErbB
Predicted BLMP-1
b
NHR-23
RORγ
RORα
RORβ
NHR-85
Rev-Erbα
Rev-Erbβ
c
NHR-23
ZnF C4
Ligand Binding
160
231
392
554
588
63% Identity
18% Identity
NHR-85
ZnF C4
Ligand Binding
110
181
255
396
514
"P" Box
"D" Box
Subdomain 1 DNA Binding
Subdomain 2 Dimerization
d
AD
DB
Empty
NHR-25
NHR-85
Empty
NHR-23
NHR-25
NHR-85
Selective
Control
e
Strep
NHR-85
NHR-23
Fraction Bound
K_D = 5.8 ± 2.2nM
NHR-23 [M]
f
lin-4 Subfragment iii
DR(1)
DR(2)
ROR site
Rev-Erb site
ROR site
g
DR(1)
DR(2)
C. elegans
C. briggsae
C. remanei
C. brenneri
C. sp5
C. tropicalis
C. japonica
C. angaria
h
NHR-85
NHR-23
Competitor
WT
Widom
Wild Type lin-4 element
lin-4 element Δggtca(1)
lin-4 element Δggtca(2)
i
NHR-85
NHR-23
Small lin-4 element (51 bp)

399

400 **Fig. 2. NHR-85$^{Rev\text{-}Erb}$ and NHR-23^{ROR} form a heterodimeric complex that binds cooperatively to**
401 **regulatory elements controlling pulsatile *lin-4* transcription.** (**a**) BLMP-1, NHR-85, and NHR-23
402 bind to the *lin-4* PCE in one-hybrid assays[11]. Browser tracks showing BLMP-1, NHR-23, and NHR-
403 85 bindings sites near the *lin-4* locus. Also indicated are the major *lin-4* pri-miRNAs[13], the
404 computationally defined binding sites for each TF, and the sub-fragments of the *lin-4* PCE element
405 used in gel shifts below. The asterisk indicates the location of the direct repeats of GGTCA in the
406 PCE element. (**b**) Sequence relationships between NHR-23 and NHR-85 and human Rev-Erb and
407 ROR. (**c**) NHR-23^{ROR} and NHR-85$^{Rev\text{-}Erb}$ domain organization. (**d**) NHR-23^{ROR} and NHR-85$^{Rev\text{-}Erb}$
408 interact with each other in two-hybrid assays. (**e**) Recombinant, purified strep-NHR-85$^{Rev\text{-}Erb,}$ and
409 NHR-23^{ROR} interact in MST binding assays. (**f**) Sequences of the PCE sub-fragment iii from a and the
410 51bp minimal binding element (grey box) derived from *lin-4* PCEiii. (**g**) Conservation of the direct
411 repeats DRs in the PCE elements of different nematode species. (**h** and **i**) EMSA experiments of wild-
412 type and mutant target DNAs using recombinant NHR-85$^{Rev\text{-}Erb}$ and NHR-23^{ROR}.
413

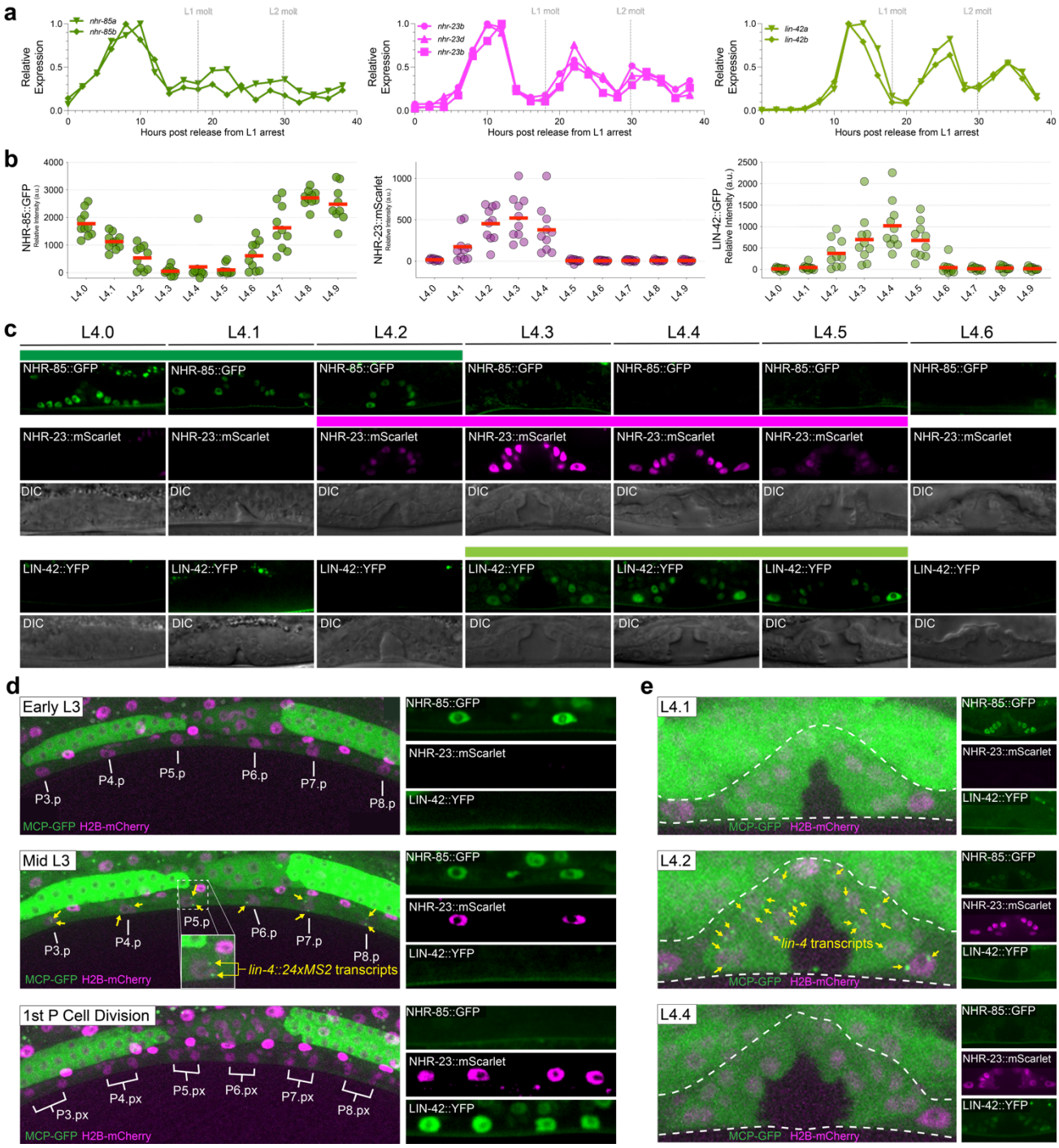

Fig. 3. *lin-4* transcription occurs during the brief periods where NHR-85$^{Rev\text{-}Erb}$::GFP and NHR-23^{ROR}::mScarlet are co-expressed. (**a**) RNA-seq time course data of *nhr-85, nhr-23,* and *lin-42* mRNA expression patterns[3]. (**b-c**) Quantification and micrographs depicting NHR-85$^{Rev\text{-}Erb}$::GFP, NHR-23^{ROR}::mScarlet, and LIN-42^{Period}::YFP expression in hypodermal seam cells and vulval cells, respectively, in each morphologically defined L4 substage[25]. Circles in b represent average

421 measurements from individual animals (3 cells sampled); red bars indicate the mean. Colored bars
422 indicate ranges of detectable expression. (**d**) Time course experiments demonstrate that *lin-*
423 *4::24xMS2* expression occurs immediately before the first Pn.p cell divisions and not until NHR-85^{Rev-}
424 ^{Erb}::GFP are NHR-23^{ROR}::mScarlet are co-expressed in the VPCs. *lin-4::24xMS2* expression
425 terminates by the time NHR-85$^{Rev-Erb}$::GFP expression is extinguished around the time of the first VPC
426 division. (**e**) Dynamic *lin-4::24xMS2* transcription also correlates with NHR-85$^{Rev-Erb}$::GFP/ NHR-
427 23^{ROR}::mScarlet in the L4 stages of vulval development.
428

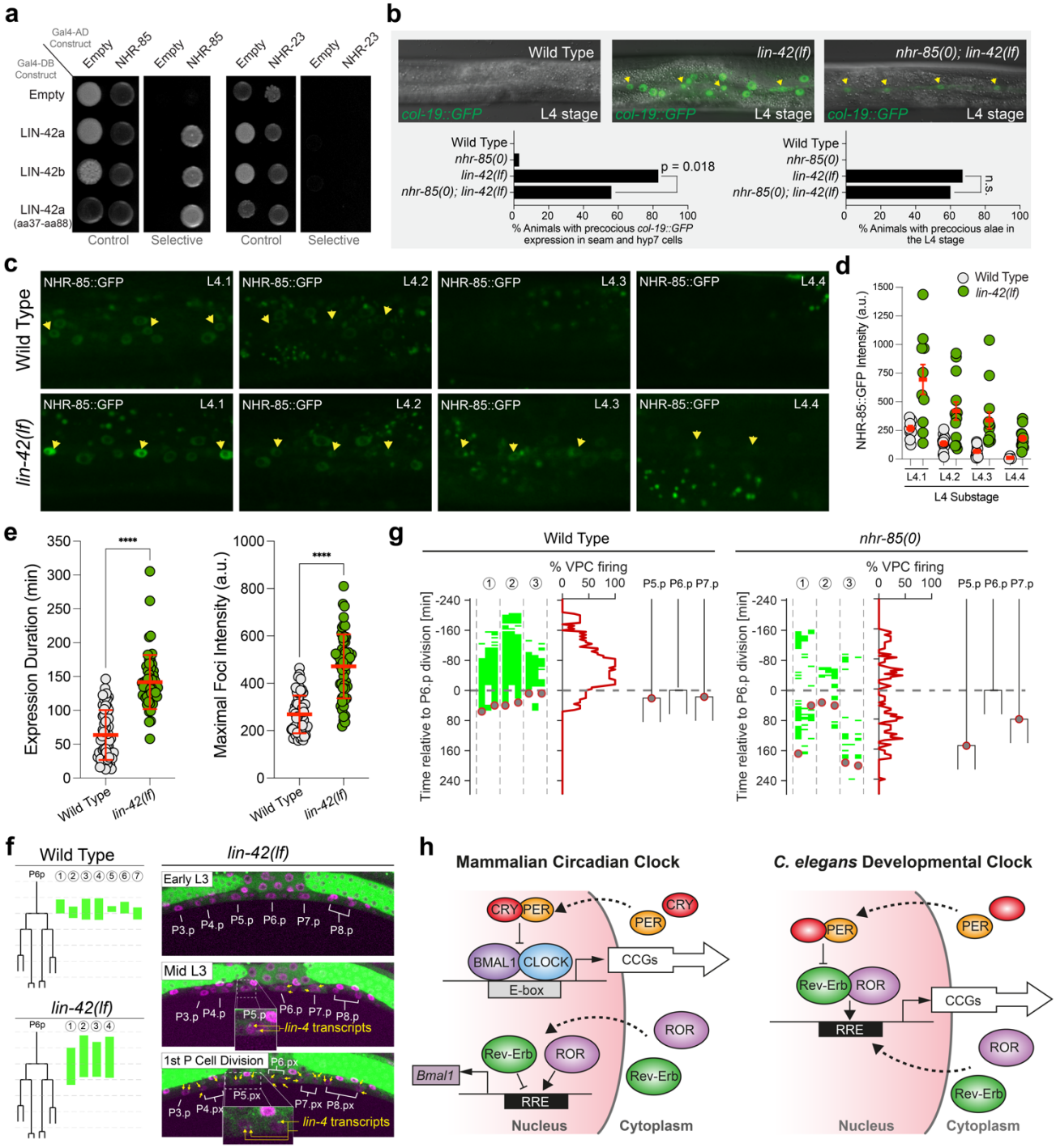

Fig. 4. LIN-42^{Period} binds to and regulates the expression dynamics of NHR-85 to control the amplitude and duration of *lin-4* transcription. (**a**) LIN-42 isoforms interact with NHR-85$^{Rev\text{-}Erb}$ but not NHR-23^{ROR} in two-hybrid assays. (**b**) *lin-42(lf)* mutants express *col-19::GFP* during the L3 stage of development and deletion of *nhr-85(0)* suppresses these phenotypes. Yellow arrows indicate the

435 lateral seam cells of L4-staged animals. Error bars were calculated using two-tailed chi-square
436 analysis. (**c and d**) Representative images and quantification of NHR-85$^{Rev\text{-}Erb}$::GFP expression
437 dynamics in hypodermal cells of L4-staged wild-type and *lin-4(lf)* animals. Yellow arrows indicate the
438 lateral seam cells of L4-staged animals. Circles represent the average expression in three seam cells
439 of an individual animal. Error bars show mean and standard deviation. Significance was calculated
440 using Welch's t-test. (**E**) Quantification of the duration and intensity of MCP-GFP foci in L3-staged
441 animals. Error bars and significance are calculated as in d. (**f**) Time course analysis of the onset/offset
442 times for MCP-GFP foci in VPCs of wild-type and *lin-42(lf).* Green lines indicate the timing of *lin-*
443 *4::24xMS2* expression in P6.p cells of individual animals. Pictographs show a representative image
444 of the ventral surface of a single *lin-42(lf)* animal throughout the time course. (**g**) High-resolution time
445 course analysis of *lin-4::24xMS2* expression in wild-type and *nhr-85(0)* mutants, aligned to first P6.p
446 cell division (t=0). Green areas indicate detectable MCP-GFP foci in individual P cells (P5.p – P7.p)
447 (n = 3 animals). Grey circles represent the timing of the P5.p and P7.p divisions. (**h**) Model of the
448 mammalian circadian clock and the *C. elegans* developmental clock uncovered in this study.